Journal of Anesthesia (2024) 38:232–243
https://doi.org/10.1007/s00540-023-03305-1

ORIGINAL ARTICLE

Targeted local anesthesia: a novel slow-release Fe_3O_4–lidocaine–PLGA microsphere endowed with a magnetic targeting function

Ling-xi Zheng[1] · Qian Yu[1] · Qiang Li[2] · Chuan-dong Zheng[1,2]

Received: 28 June 2023 / Accepted: 25 December 2023 / Published online: 4 February 2024

Abstract

Purpose Lidocaine microspheres can prolong the analgesic time to 24–48 h, which still cannot meet the need of postoperative analgesia lasting more than 3 days. Therefore, we added Fe_3O_4 to the lidocaine microspheres and used an applied magnetic field to attract Fe_3O_4 to fix the microspheres around the target nerves, reducing the diffusion of magnetic lidocaine microspheres to the surrounding tissues and prolonging the analgesic time.

Methods Fe_3O_4–lidocaine–PLGA microspheres were prepared by the complex-emulsion volatilization method to characterize and study the release properties in vitro. The neural anchoring properties and in vivo morphology of the drug were obtained by magnetic resonance imaging. The nerve blocking effect and analgesic effect of magnetic lidocaine microspheres were evaluated by animal experiments.

Results The mean diameter of magnetically responsive lidocaine microspheres: 9.04 ± 3.23 μm. The encapsulation and drug loading of the microspheres were 46.18 ± 3.26% and 6.02 ± 1.87%, respectively. Magnetic resonance imaging showed good imaging of Fe_3O_4–Lidocain–PLGA microspheres, a drug-carrying model that slowed down the diffusion of the microspheres in the presence of an applied magnetic field. Animal experiments demonstrated that this preparation had a significantly prolonged nerve block, analgesic effect, and a nerve anchoring function.

Conclusion Magnetically responsive lidocaine microspheres can prolong analgesia by slowly releasing lidocaine, which can be immobilized around the nerve by a magnetic field on the body surface, avoiding premature diffusion of the microspheres to surrounding tissues and improving drug targeting.

Keywords Magnetic attraction · Superparamagnetic iron oxide nanoparticles · Local anesthetics · Slow-release · Long-action analgesia

Abbreviations

PLGA	Poly (lactic-co-glycolic acid)
PVA	Polyvinyl alcohol
DCM	Dichloromethane
PBS	Phosphate-buffered saline
SEM	Scanning electron microscopy
TEM	Transmission electron microscopy
UV	Ultraviolet
CTMR	Cutaneous trunk reflex
MRI	Magnetic resonance imaging

✉ Chuan-dong Zheng
zhengchuandong@swjtu.edu.cn

[1] Institute of Biomedical Engineering, College of Medicine, Southwest Jiaotong University, Chengdu 610031, Sichuan, China

[2] Department of Anesthesiology, The Third People's Hospital of Chengdu, Affiliated Hospital of Southwest Jiaotong University, 19 Yangshi Street, Qingyang District, Chengdu 610031, Sichuan, China

Introduction

To accommodate the long-duration postoperative analgesia period, which usually requires continuous use of local anesthetics for at least 48–72 h, the duration of action of local anesthetics needs to be prolonged as much as possible [1]. This can be achieved via methods, such as addition of adjuvants, nerve catheter placement, and repeated blocks, but each of these methods has its own disadvantages. A new approach to improve the duration of action of local anesthetics is to add a casing or carrier to the local anesthetic to achieve a slow or on-demand release effect and prolong the duration of continuous analgesia. This method of drug delivery first emerged in targeted therapy

for oncology and is called a novel drug delivery system [2–4]. The advantage of novel drug delivery systems is their ability to reduce drug accumulation and which extend the time a drug is active in the body [5–8].

Many studies have employed Poly lactic-polyglycolic acid (PLGA) loading of drugs to achieve slow release [9]. PLGA microspheres release the drug by two mechanisms [10]: diffusion and degradation. Diffusion is the dissolution of the drug and diffusion of the solution into the microspheres through the microsphere voids, which is the main mode of sustained release of the microspheres. Degradation is the release of the drug along with the dissolution of the PLGA shell. Unlike other studies that have combined PLGA with lidocaine to prolong the duration of analgesic action [11]. The present study used magnetic microspheres loaded with local anesthetic and attached a specific magnetic field strength to the nerve body projection to anchor the microspheres around the nerve and avoid premature diffusion of the microspheres into the surrounding tissue, resulting in decreased analgesia time.

In recent years, scholars have conducted a series of studies on local anesthetic retardants, but these studies did not address the free diffusion of local anesthetic microsphere retardants after local injection. This study designed, prepared, and characterized magnetically responsive lidocaine microspheres in order to address the problem of diffusion of local anesthetic microsphere formulations into surrounding tissues. In addition, we used magnetic resonance imaging (MRI) to study the anchoring effect of magnetic lidocaine microspheres on nerves. Animal experiments were used to study the nerve blocking effect and sustained analgesic time of magnetic lidocaine microspheres.

Methods

Reagents and materials

Nano-iron oxide (Fe_3O_4) was purchased from the Aladdin Biochemical Technology Co. (Shanghai, China). Lidocaine hydrochloride was purchased from McLean Biochemical Technology Co. (Shanghai, China). Polylactic acid (PLGA; 50:50, MW 500–15,000) polymers were purchased from Dagang Biological Engineering Co. (Jinan, China). Gelatin was purchased from Sigma–Aldrich (Germany).

Polyvinyl alcohol (PVA) was purchased from Kearon Chemicals Co. (Chengdu, China). Dichloromethane (DCM) was purchased from the Kelong chemical reagent factory (Chengdu, China). The laboratory provided 25% urethane injection, deionized water, and 0.9% physiological saline.

Synthesis of Fe_3O_4–lidocaine–PLGA and blank microspheres

Fe_3O_4–lidocaine–PLGA microspheres were prepared using a $W_1/O/W_2$ emulsifying-solvent evaporation technique. First, 0.25 g of gelatin was weighed and dissolved in 25 mL deionized water and stirred at a constant temperature of 50 ℃ for 10 min to fully dissolve. Next, 0.1 g of Fe_3O_4 nanoparticles were weighed into 2 mL 1% gelatin and ultrasonicated for 10 min. Furthermore, lidocaine (0.1 g) was weighed and dissolved in 2 mL deionized water to form a 5% lidocaine solution, and 2 mL Fe_3O_4-1% gelatin was added to form the internal aqueous phase, W_1. Further, 0.4 g of PLGA was weighed and dissolved in 8 mL DCM to form the oil phase, O. The internal aqueous phase, W_1 was pipetted into the oil phase, O at a controlled drop rate of 40 drops/min. Next, the internal aqueous phase, W_1 was slowly added to the oil phase, O with a pipette gun at a rate of 40 drops/min and dispersed for 5 min using a high-speed homogenizer at 8000 rpm to form stable colostrum, W_1/O. In addition, PVA (1.5 g) was weighed and dissolved in 50 mL deionized water with stirring at a constant temperature of 90 °C for 40 min to fully dissolve and left for 1 h to eliminate foam and was configured as the external aqueous phase, W_2. Under stirring at 800 rpm, colostrum was added dropwise into the external aqueous phase, W_2, and dispersed at 8000 rpm for 5 min in a high-speed homogenizer to form the stable milk compound, $W_1/O/W_2$. The mixture was stirred at room temperature to evaporate the organic solvent completely. The mixture was centrifuged at 3000 rpm/min (4 °C) for 5 min, centrifugation radius = 15 cm, washed three times, and lyophilized to obtain a brown powder (Fig. 1). Blank microspheres were prepared by simply replacing 2 mL of 5% lidocaine solution with 2 mL of deionized water to obtain blank microspheres.

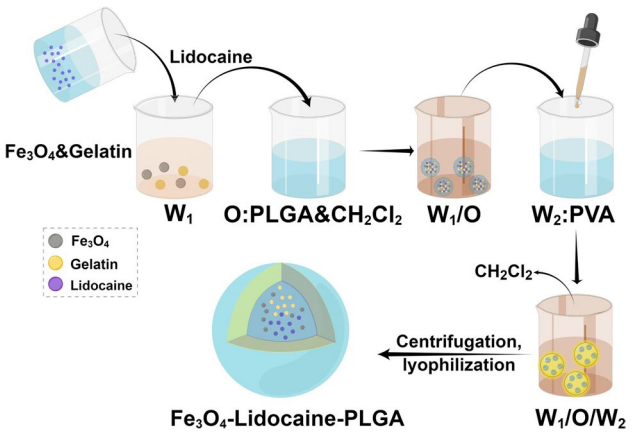

Fig. 1 Schematic diagram of the preparation process of Fe_3O_4–lidocaine–PLGA microspheres. PLGA, poly(lactic-co-glycolic acid). By Figdraw

Characterization of Fe_3O_4–lidocaine–PLGA microspheres

An appropriate amount of microsphere powder was added to deionized water and ultrasonically dispersed before measurement. The particle morphology was characterized using transmission electron microscopy (TEM, FEi-F20, Fei Co., USA) and scanning electron microscopy (SEM, SU5000, Hitachi Co., Tokyo). The magnetic response parameters of the microspheres under magnetic fields were measured using a vibrating sample magnetometer (VSM, Lakeshore-7404, Lake Shore Co., USA) to obtain the hysteresis curves.

In vitro drug release study

Establishment of the standard curve for lidocaine hydrochloride

Lidocaine hydrochloride (10 mg) was dissolved in phosphate buffered saline (PBS) solution to achieve a concentration of 1 mg/mL lidocaine hydrochloride solution. Lidocaine hydrochloride was diluted into 5, 10, 20, 40, and 80 μg/mL solutions, and the absorbance values at 263 nm were measured by ultraviolet (UV)-visible spectrophotometer to plot the standard curve of lidocaine hydrochloride concentration (C)-absorbance value (A).

In vitro release profile of Fe_3O_4–lidocaine–PLGA microspheres

In this analysis, 30 mg of lidocaine–Fe_3O_4–PLGA nano microspheres were weighed precisely and placed in a centrifuge tube containing 30 mL of PBS solution (pH 7.4). The solution was classified into a magnetic field group and a non-magnetic field group, and a 120 mT static magnetic field was applied outside the magnetic field group. The centrifuge tubes of both groups were placed on a constant temperature water bath shaker at 37 °C with an oscillation frequency of 100 times/min. The supernatant (2 mL) was collected at 0.5, 1, 2, 4, 8, 12, 24, 48, and 60 h, respectively, and the absorbance was measured at 263 nm using a UV spectrophotometer. Next, 2 mL of PBS was added, and the concentration of lidocaine hydrochloride was calculated according to its standard curve at the corresponding time. The concentration of lidocaine at the corresponding time was calculated according to the standard curve of lidocaine hydrochloride. The cumulative amount of drug released at each time point was measured, and the in vitro release curve was plotted.

Drug loading and encapsulation rate

In this study, 10 mg of Fe_3O_4–lidocaine–PLGA was precisely weighed in a volumetric flask, and 5 mL of DCM was added to dissolve and impair the microspheres. Deionized water was added and centrifuged to remove the shell and Fe_3O_4, and the volume was fixed. The absorbance was measured at 263 nm using a UV–visible spectrophotometer, and the mass of lidocaine hydrochloride in the solution was calculated using the equation for the standard curve of lidocaine hydrochloride. The drug-loading and encapsulation rates of lidocaine hydrochloride were calculated using Eqs. (1) and (2):

$$\mathrm{LE}\% = \frac{W_e}{W_m} \times 100\% \tag{1}$$

$$\mathrm{EN}\% = \frac{1 - C_f}{C_t} \times 100\% \tag{2}$$

Animals

Specific pathogen-free New Zealand rabbits (3000–3500 g; 24 males) were provided by the animal experiment center at the West China Hospital of Sichuan University. The rabbits were 5–6 months old and routinely kept at an indoor temperature with unlimited access to food and water. Specific pathogen-free male Sprague–Dawley rats (250–300 g) were purchased from Dossy Experimental Animal Co., LTD (CN). The rats were housed under the same conditions, which also entailed room temperatures of 24 °C, relative humidity controlled at 50%, and a cycle of 12 h of darkness and 12 h of light. The sample size calculation was carried out by the program GLIMMPSE 3.1.0, and sample size calculation of repeated measures was carried out by program, which was introduced by Guo et al. [12]. The peripheral nerve block experiment is taken as an example: after opening the program, corresponding parameters according to the page guidelines and experimental design requirements were filled. When the type I error rate (α) was 0.01, the total sample size calculated was 20 rabbits divided into 4 groups ($n = 5$). The Institutional Animal Care and Use Committee approved all animal study protocols at the West China Hospital of Sichuan University (ethical approval number: 20230307006).

Peripheral nerve block and analgesia experiment

Establishing the sciatic nerve model

Rabbits received an intravenous injection of 25% uratan (5 mL/kg) into their ear margins until their corneal reflexes

disappeared. Each rabbit was placed in the lateral position, the limbs were fixed, the hair of the left lower limb and buttocks were removed, the projection of the sciatic nerve of the left lower limb was taken, and a 3.5 cm long incision was made along the midline. The muscles were dissected at the sciatic fossa, and the sciatic nerve was located. A glass needle was used to gradually dissect the nerve downward to fully expose the nerve. Two sets of stimulation electrodes (one set of blue wires and one set of pink wires) were wrapped around the nerve at 1–1.5 cm, and extreme caution was exercised during the installation of the stimulation electrodes to avoid damage to the nerve. Moreover, the stimulation electrodes needed to be properly secured to avoid the groups of wires coming into contact and causing a short circuit. After installing the electrodes, the head end of the catheter was placed at the sciatic nerve. The tail end of the catheter was assembled with a heparin cap and properly secured, and then the catheter was sealed by injecting 0.9% saline into the catheter with a syringe for each group of rabbits (Fig. S1). The tissues and incisions were sutured layer-by-layer, and the wound was covered with gauze. Upon the return of corneal reflexes of the rabbits, muscle tone recovery of the lower limbs on the operated side was observed, and the rabbits were subsequently returned to the cage for rearing (two/cage). All rabbits were fed ad libitum. Criteria for successful preparation of the sciatic nerve model were: the electrical activity signal of the nerve was detected by stimulating the electrode fixed in the lower limb using the BL-420i biosignal processing system, and the muscle pulsation of the rabbit's lower limb was also visible.

In vivo morphology of magnetic lidocaine microspheres in rabbits

Nano-Fe_3O_4 with superparamagnetic properties is a good MRI contrast agent [13]. We used MRI to obtain in vivo images of magnetic lidocaine microspheres based on this property. Four New Zealand rabbits were selected and divided into four groups, one in each group. Images of each of the four rabbits with two sets of stimulation electrodes and drug injection catheters were obtained according to the "Establishment of sciatic nerve model" method.

(1) Magnetic lidocaine microspheres group (PL group): 2 g of Fe_3O_4–Lidocaine–PLGA microspheres were dispersed in 2 mL of 0.9% saline, injected into the catheter, and the magnet was fixed to the lower limb on the surgical side of the rabbit. The magnet was temporarily removed for MRI. (2) Lidocaine–PLGA microspheres group (PNM group): 2 g Fe_3O_4–Lidocaine–PLGA microspheres were dispersed with 2 mL of 0.9% saline, injected through the catheter, and no magnet was set. (3) Lidocaine group (L group): 2 mL of Lidocaine containing the same content as that in the PL group was injected through the catheter and the magnet was set in the same way as in the PL group. (4) Blank microsphere group (BM group): 2 g of blank microspheres (Fe_3O_4–PLGA microspheres) were dispersed in 2 mL of 0.9% saline, injected via catheter, and the magnet was set in the same way as the PL group.

MRI pictures of groups PL, PNM, and BM were taken 2 and 8 h after drug administration, respectively. Considering the action time of lidocaine, MRI pictures of the L group were taken 15 min and 2 h after administration, respectively.

Evaluation of nerve block efficacy and lower limb movement

The experimental animals were divided into four groups of five animals each using the random number table method. Each group was treated as follows: (1) magnetic lidocaine microsphere group (PL group): 2 mL of saline was used to disperse 2 g of magnetic lidocaine microsphere powder, injected via catheter, and a magnet was properly fixed on the lower limb of the surgical side of the rabbit (Magnetic elastic bandages are shown in Fig. S1D); the static magnetic field was 120 mT, and the magnet was withdrawn after 60 h. (2) Lidocaine–PLGA group (PNM group): 2 g of Fe_3O_4–lidocaine–PLGA microspheres were solubilized in 2 mL of saline and injected through a catheter without the magnet settings. Each gram of microspheres contained 0.0602 g of lidocaine. (3) Physiological saline control group (C group): 2 mL of 0.9% physiological saline injected via catheter, and the magnet was set as before. (4) Blank microsphere group (BM group): 2 g of blank microspheres were dispersed in 2 mL of 0.9% physiological saline, injected via catheter, and the magnet was set as before.

The complex action potentials and conduction velocities of the sciatic nerve trunk were measured before (T_0) and 30 min (T_1), 2 h (T_2), 8 h (T_3), 16 h (T_4), 24 h (T_5), 48 h (T_6), 60 h (T_7), 62 h (T_8), and 64 h (T_9) after drug injection and toe tension, then the modified Tarlov score were calculated [14]. The time difference between two successive electrical signals recorded at each time node was used to calculate the nerve conduction velocity. Furthermore, lower-extremity movements were assessed simultaneously. The toe opening reflex was scored as follows: the author pinched the skin of the rabbit's neck, lifted it off the ground, quickly lowered it but did not let it hit the ground, and observed the toe opening on the affected side. If the toe opening was not visible at all, a score of 1 was recorded; if only a mild toe opening was visible, a score of 2 was recorded; if the toe opening was clearly visible but the magnitude was still below normal, a score of 3 was recorded; and if the toe opening was completely normal, a score of 4 was recorded. In addition, the modified Tarlov score was combined with the following scoring methods and criteria: rabbits were placed on a manipulative table, and their reactions were observed by needling the ankles

with acupuncture needles. They were then placed on a spacious laboratory floor and allowed to walk freely to observe their gait. The scoring criteria were as follows: (0) complete inability to move the limb and no response to acupuncture; (1) slight response visible after acupuncture; (2) voluntary movement of all joints and no resistance when the foot was passively flexed; (3) obvious resistance when the foot was passively flexed, but the walking gait was unstable; and (4) normal walking gait.

Assessment of analgesic efficacy

Mechanical stimulus test

The cutaneous trunk reflex (CTMR) model [15, 16] is an established model for evaluation of cutaneous analgesic effects. Eighteen rats were randomly divided into three groups ($n = 6$): the 0.9% saline group (S1 group); Fe_3O_4–Lidocaine–PLGA containing 6% lidocaine (including the M1 group, with an applied magnetic field; and the NM1 group, without an applied magnetic field). The hair on the thoracolumbar segment and back of the rats in each group was removed, and each group was injected subcutaneously with 0.5 mL of the corresponding drug to form a uniformly sized wind cluster at the injection site. This edge was marked with a marker. An elastic bandage was used and a magnet was secured to the administration site on the back of the rat (the magnetic elastic bandage is similar to this secured to the rabbit). The skin trunk reflex was assessed by pinprick response using a 26-ga needle at 0 min, 30 min, 2, 4, 8, 16, 24, 36, 48, 60, 62, and 64 h after injection. Six equal-intensity pinprick stimuli were randomly applied inside the wind mass, the number of times a CTMR response could be observed was recorded, and the number of times the CTMR reaction was not energized into the inhibition rate (IR%). Calculation formula: IR% = (1 − number of CTMR responses/6) × 100%.

Hot plate test

The RB-200 intelligent hot plate instrument was used to thermally stimulate the rats. The rats were placed on the glass cover of the instrument, which was set at 55 ± 0.5 °C. Licking the hindfoot or lifting the foot was used as the pain response indicator. Inclusion criteria were pain thresholds of 5–30 s. Rats were screened one day in advance, and the pain threshold of each rat was measured and recorded. Twenty-one rats were randomly divided into three groups ($n = 7$), including the 0.9% saline group (S2 group) and Fe_3O_4–Lidocaine–PLGA containing 6% of lidocaine (including the M2 group, with an applied magnetic field; and the NM2 group, without an applied magnetic field). The rats were injected with 0.2 mL of the corresponding drugs at the sole of the right hind foot, and the groups were marked with different color markers. Immediately after the injection of the drug, the rats were returned to their cages and allowed to eat and drink freely. The group with the magnetic field removed the bedding and placed magnets with a thickness of 10 mm flat on the bottom of the rat cages. When the rat moves, the sole of the rear foot will always be in contact with the magnets. The maximum thermal stimulation time was 60 s to avoid burning the animals. The pain thresholds of the rats in each group were measured at 30 min, 2, 4, 8, 16, 24, 48, 60, 62, and 64 h after the administration of the drugs.

Statistical analysis

The experimental results were expressed as mean ± standard deviation, and $P < 0.05$ was considered statistically significant. Between-group comparisons of multiple data sets were made using Repeated Measures ANOVA and Tukey's test. All in vivo experimental data were analyzed using GraphPad Prism (version 9.1.0, GraphPad Software, San Diego, CA, USA).

Results

Characterization of Fe_3O_4–lidocaine–PLGA

Fe_3O_4–lidocaine–PLGA was prepared using the compound-emulsion volatilization method; it appeared as a brown powder to the naked eye (Fig. 2C1). The morphology and internal structure of the microspheres were observed by SEM and TEM. The results showed that the average particle size of Fe_3O_4–lidocaine–PLGA microspheres was 9.04 ± 3.23 μm (Sample number = 5), and the iron tetroxide nanoparticles and drugs wrapped under the PLGA shell were visible (Fig. 2A).

Verification of superparamagnetism

As shown in Fig. 2B, the magnetic hysteresis lines of Fe_3O_4–lidocaine–PLGA microspheres were S-shaped with a saturation magnetization intensity of 0.9–1.0 emu/g at room temperature. When the additional magnetic field was removed, the hysteresis return line passed through the point (0, 0), and the magnetic field intensity was 0. These results suggested that the coercivity of the Fe_3O_4–lidocaine–PLGA microspheres was equal to the residual magnetization intensity, both of which were zero, and no hysteresis occurred. Therefore, the Fe_3O_4–lidocaine–PLGA microspheres were superparamagnetic. In addition, magnetic lidocaine microspheres could be attracted to magnets and swim (Fig. 2C2).

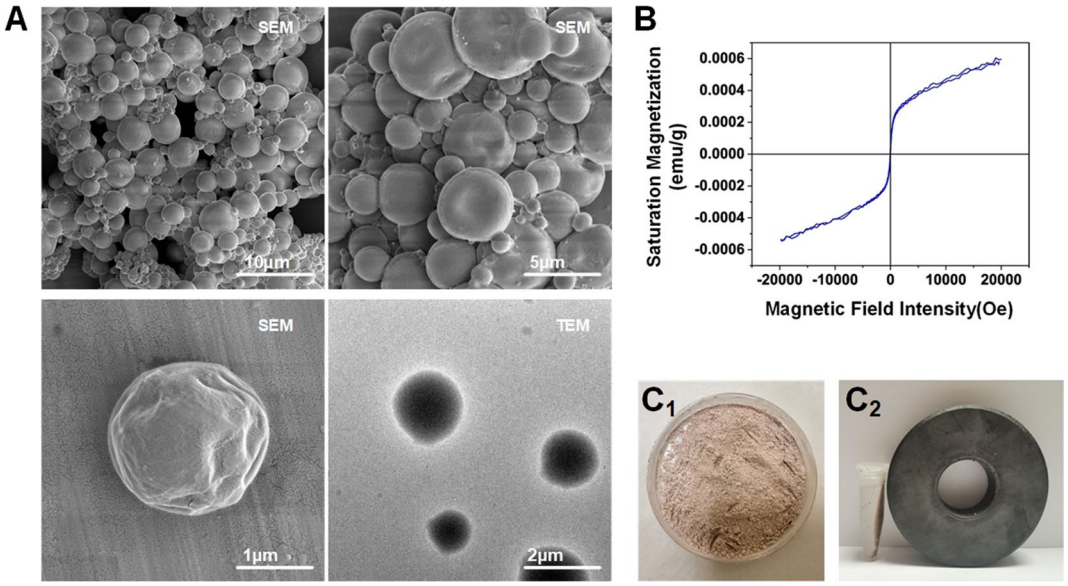

Fig. 2 SEM and TEM characterization and magnetic verification of lidocaine microspheres **a** Magnetic lidocaine microspheres as observed on SEM at ×1000, ×5000, and ×10,000 TEM. **b** Hysteresis lines of magnetic lidocaine microspheres. **c** Naked-eye view of magnetic lidocaine microsphere powder, and its swimming motion under the attraction of a magnet. *SEM* scanning electron microscopy, *TEM* transmission electron microscopy

Sustained release of lidocaine in vitro

Figure 3B shows the in vitro release profile of the Fe_3O_4–lidocaine–PLGA microspheres. After 60 h, cumulative lidocaine hydrochloride release was 97 ± 1.97%. The concentration (C) − absorbance (A) standard curve of the lidocaine hydrochloride solution (Fig. 3A) was converted to show that the encapsulation rate of Fe_3O_4–lidocaine–PLGA microspheres was 46.18 ± 3.26%, and drug loading was 6.02 ± 1.87% (Sample number = 5). The results were similar to the encapsulation rate in the Wang et al. study [17].

In vivo morphology of magnetic lidocaine microspheres in rabbits

As shown in Fig. 4, no significant diffusion was shown in the PL and BM groups at 2 and 8 h after administration. While the PNM group was slightly diffused 2 h after administration, more obvious diffusion was apparent 8 h after administration. The L group displayed more obvious diffusion 15 min and 2 h after administration.

Time regularity of nerve block in the peripheral nerve model

Nerve action potential and nerve conduction velocity

As shown in Fig. 5, sciatic nerve action potential amplitude and nerve conduction velocity decreased in the PL group from 30 min to 62 h after drug administration compared with the BM and C groups ($P < 0.05$). We also observed that the sciatic nerve action potential amplitude and nerve conduction velocity in the PNM group were essentially parallel to the results in the PL group from 30 min to 2 h after

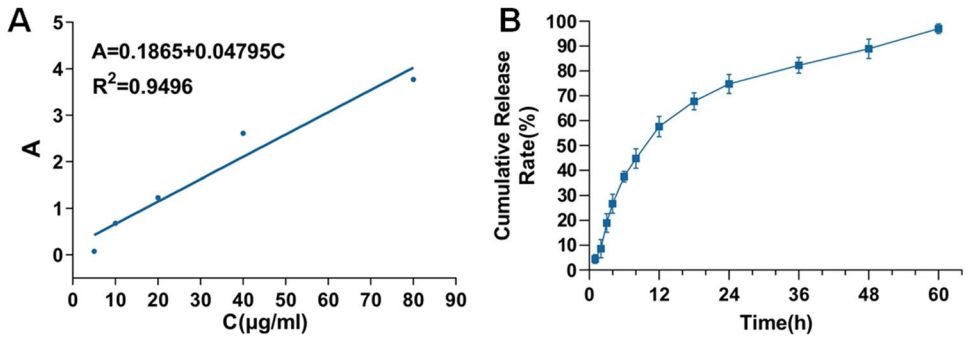

Fig. 3 In vitro release assay. **a** Concentration–absorbance standard curve of lidocaine hydrochloride solution. **b** In vitro release curve of magnetic lidocaine microspheres

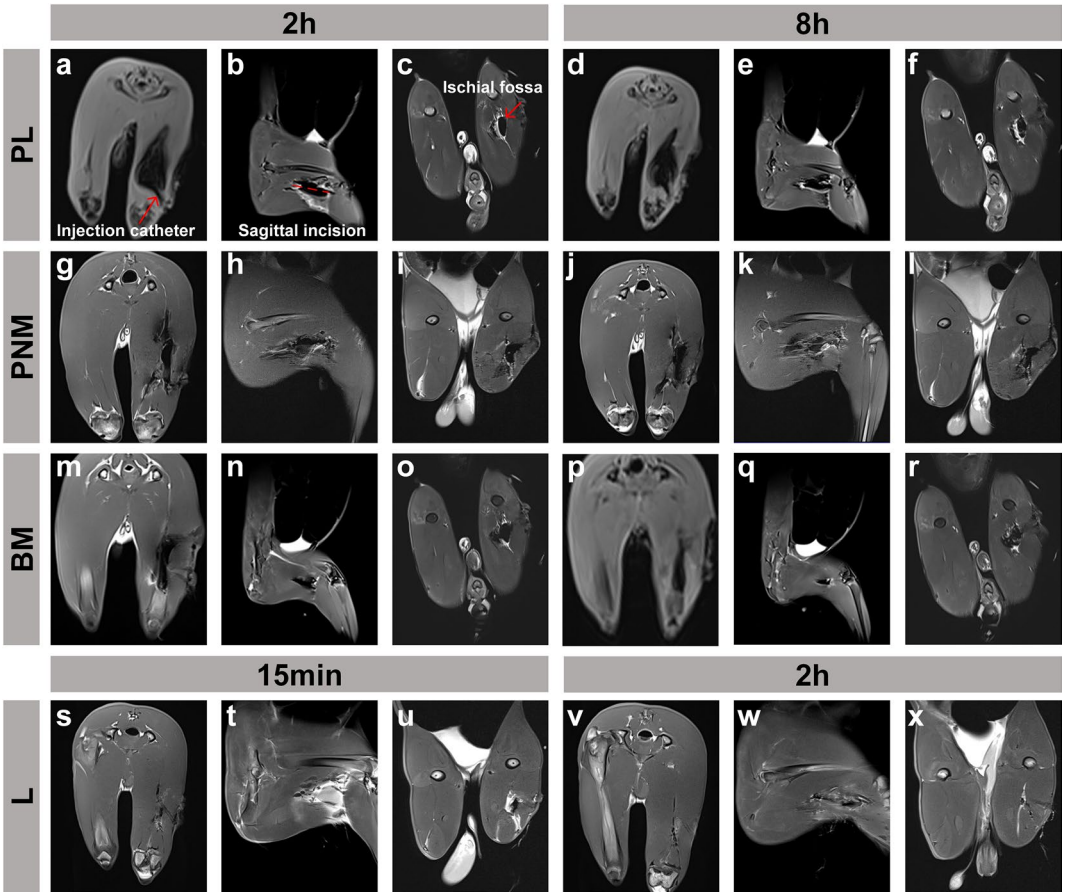

Fig. 4 Magnetic resonance imaging (MRI) of the distribution of each group of drugs injected into rabbits' periphery of the sciatic nerve. In each group of rabbits, a sagittal incision was made at the sciatic fossa of the right lower limb, and a drug delivery catheter injected the drug around the sciatic nerve. Refer to PL group-2 h for the legend of the site of administration and type of incision. **a**–**c** MRI of the PL group in rabbits at 2 h; **d**–**f** MRI of the PL group in rabbits at 8 h; **g**–**i** Magnetic resonance imaging of the PNM group in rabbits at 2 h; **j**–**l** MRI of the PNM group in rabbits at 8 h; **m**–**o** MRI of the BM group in rabbits at 2 h; **p**–**r** MRI of the BM group in rabbits at 8 h; **s**–**u** MRI of the L group in rabbits at 15 min; **v**–**x** MRI of the L group in rabbits at 2 h

drug administration. However, from the 8 h, the nerve action potential and conduction velocity of the sciatic nerve in the PL group were lower than those in the PNM group. At 48 h, the nerve action potentials and conduction velocity of the sciatic nerve in the PNM group were close to those in the C and BM group. In contrast, the nerve block effect in the PL group lasted up to 62 h, which was different from that in the PNM group ($P < 0.05$), which may suggest that magnetic lidocaine microspheres can be anchored around the nerve by a magnetic field to reduce diffusion, thus exhibiting a longer duration of nerve block effect.

Toe tension reflex score and modified Tarlov score

As shown in Fig. 6, the toe-tension reflex score and modified Tarlov score of the BM and C groups were maintained at about 4 before and after drug administration. However, toe-tension reflex and modified Tarlov scores were lower in the PL group than in the BM and C groups 30 min–62 h after drug administration ($P < 0.05$). We also observed that from 30 min to 2 h after drug administration, the toe-tension reflex and modified Tarlov scores of the PNM group were essentially parallel to those of the PL group. However, from 8 h, the toe-tension reflex and modified Tarlov score of the PNM group began to rise gradually. After 48 h, the PNM group was functionally parallel to the results of the BM and C groups. These results suggest that magnetic lidocaine microspheres may be able to produce a nerve block for a longer duration.

Assessment of analgesic efficacy

Mechanical stimulus test

The results of CTRM inhibition in each group are shown in Table 1. As shown in Fig. S2, at 30 min the magnetically

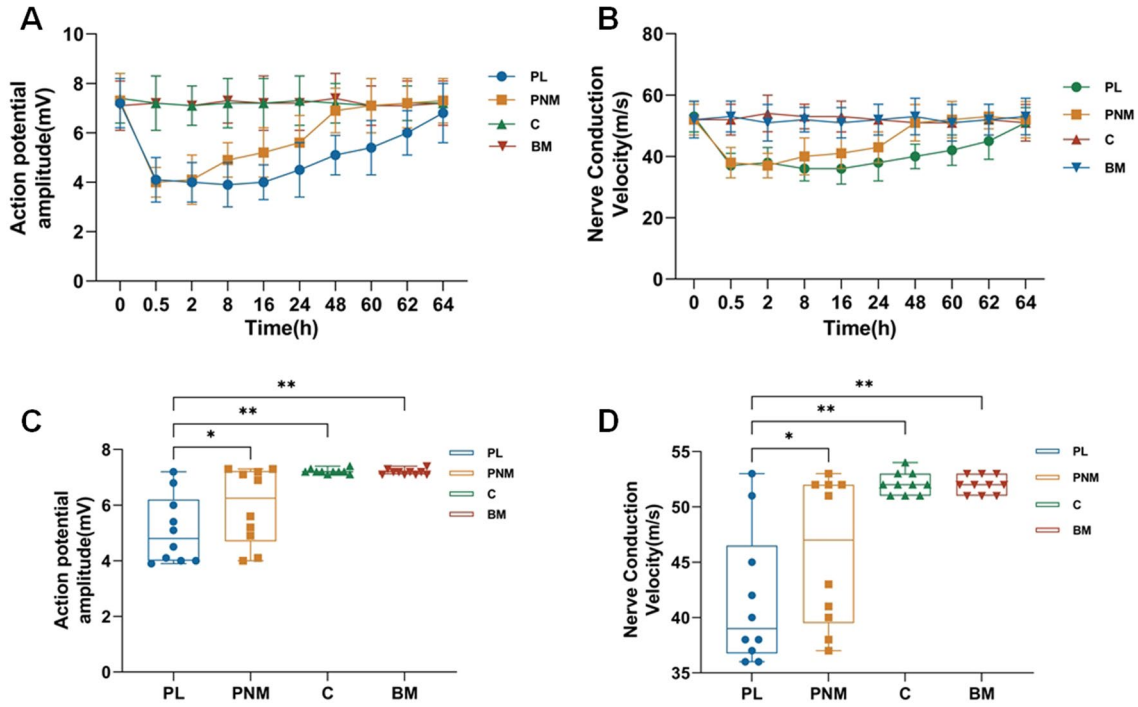

Fig. 5 The blocking effects of PL, PNM, C, and BM groups on the rabbit sciatic nerve. **a** Trends of sciatic nerve action potential amplitude at each time point in each group. **b** Trends of sciatic nerve conduction velocity at each time point in each group. **c** *Box* diagram of action potential amplitude for each group. **d** *Box* plots of nerve conduction velocity for each group. **c**, **d** Comparison of action potential amplitude and nerve conduction velocity of the sciatic nerve at each time point in each group using one-way analysis of variance (one-way ANOVA) and Tukey's test. Amplitude and nerve conduction velocity of the sciatic nerve in each group at each time point. Data are expressed as mean ± standard deviation. Statistical significance: $^{*}P < 0.05$, $^{**}P < 0.01$

responsive lidocaine microspheres completely inhibited the cutaneous trunk reflex with or without the action of a peripheral magnetic field. Magnetic lidocaine without the action of a peripheral magnetic field began to decline at 4 h, and the inhibition rate was already below 50% at 24 h, with the effect almost completely disappearing after 48 h. In contrast, magnetic lidocaine with a peripheral magnetic field began to start a slow decline after 4 h and still had a 72.22% inhibition rate by 24 h. The recorded inhibition effect lasted until 60 h when it was still 22.22%. These results indicate that magnetic lidocaine microspheres can prolong skin analgesia to some extent due to magnetic attraction in the presence of a peripheral magnetic field.

Hot plate test

The pain threshold of each rat was measured before administration. The mean baseline values for the three groups of rats were 10.14 ± 1.07, 10.00 ± 1.16, and 10.29 ± 0.96 s, respectively. The results for basal pain thresholds were similar to those of Malpezzi-Marinho ELA et al. [18] As shown in Fig. S3, magnetic lidocaine microspheres with or without magnetic field effect significantly relieved acute pain induced by thermal stimulation in rats from 30 min to 4 h after administration ($P < 0.0001$). After 8 h, the magnetic lidocaine microspheres without a magnetic field began to reduce the acute pain relief, and the degree of relief was significantly different from that of the M2 group ($P < 0.05$). The M2 group was still able to experience acute pain relief from pain caused by thermal stimulation to a certain extent at 64 h ($P < 0.05$). However, there was no statistical difference between the NM2 group and the control group at the 48 h ($P > 0.05$). This suggests that the time available to relieve acute pain induced by thermal stimulation was prolonged to some extent by magnetic lidocaine microspheres under the effect of the magnetic field.

Discussion

Magnetic lidocaine microspheres were prepared by the complex-emulsion volatilization method, and the feasibility was verified by characterization, verification of superparamagnetism verification, and in vitro release tests. The microspheres exhibited a single-particle, monodisperse spherical shape with an average particle size of 9.04 ± 3.23 μm under SEM, meeting the criteria for micron-sized injectable pharmaceutical formulations. The shell formed by PLGA

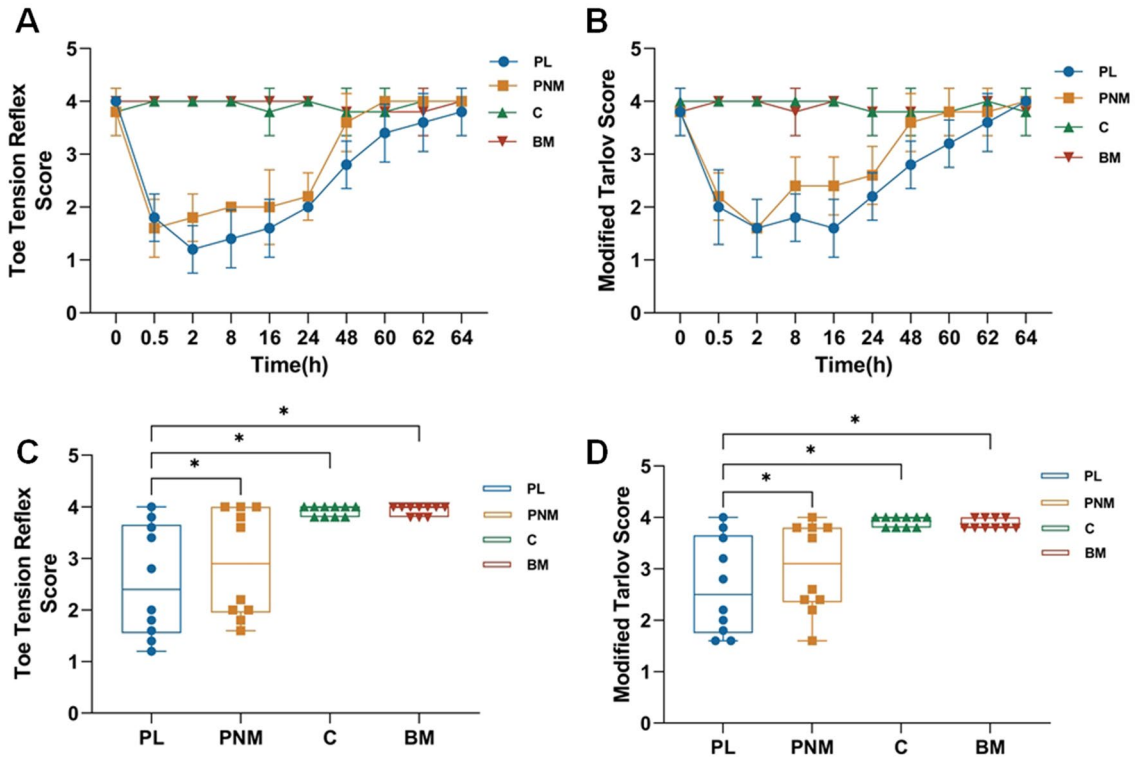

Fig. 6 Lower limb movements of rabbits in PL, PNM, C, and BM groups were assessed. **a** Trends in toe-tension reflex scores of each group at each time point. **b** Trends in modified Tarlov scores of each group at each time point. **c** *Box* plots of toe-tension reflex scores for each group. **d** *Box* plots of modified Tarlov scores for each group. **c**, **d** Toe tension reflex scores and modified Tarlov scores of each group were analyzed by using one-way analysis of variance (one-way ANOVA) and Tukey's test. Statistical significance is shown: $^{*}P < 0.05$

Table 1 Results of cutaneous trunk reflex inhibition in each group (Mean ± SD)

Time	M1		NM1		S1	
	NI	IR%	NI	IR%	NI	IR%
Before	0.00 ± 0.00	0.00 ± 0.00%	0.00 ± 0.00	0.00 ± 0.00%	0.00 ± 0.00	0.00 ± 0.00%
0.5 h	6.00 ± 0.00	100.00 ± 0.00%	6.00 ± 0.00	100.00 ± 0.00%	0.00 ± 0.00	0.00 ± 0.00%
2 h	6.00 ± 0.00	100.00 ± 0.00%	5.83 ± 0.41	97.22 ± 6.81%	0.00 ± 0.00	0.00 ± 0.00%
4 h	6.00 ± 0.00	100.00 ± 0.00%	6.00 ± 0.00	100.00 ± 0.00%	0.00 ± 0.00	0.00 ± 0.00%
8 h	5.67 ± 0.52	94.43 ± 8.61%	5.33 ± 0.52	88.89 ± 8.61%	0.00 ± 0.00	0.00 ± 0.00%
16 h	5.17 ± 0.75	86.11 ± 12.55%	4.17 ± 0.41	69.45 ± 6.80%	0.00 ± 0.00	0.00 ± 0.00%
24 h	4.33 ± 0.82	72.22 ± 13.61	2.83 ± 0.75	47.22 ± 12.55%	0.00 ± 0.00	0.00 ± 0.00%
36 h	3.83 ± 0.41	63.89 ± 6.81%	1.67 ± 0.82	27.78 ± 13.61%	0.00 ± 0.00	0.00 ± 0.00%
48 h	2.50 ± 0.55	41.67 ± 9.13%	0.33 ± 0.52	5.56 ± 8.61%	0.00 ± 0.00	0.00 ± 0.00%
60 h	1.33 ± 0.52	22.22 ± 8.60%	0.00 ± 0.00	0.00 ± 0.00%	0.00 ± 0.00	0.00 ± 0.00%
62 h	0.83 ± 0.75	13.89 ± 12.55%	0.00 ± 0.00	0.00 ± 0.00%	0.00 ± 0.00	0.00 ± 0.00%
64 h	0.50 ± 0.55	8.34 ± 9.13%	0.00 ± 0.00	0.00 ± 0.00%	0.00 ± 0.00	0.00 ± 0.00%

Note: Number of inhibitions (NI) and inhibition rate (IR%)

wrapped with lidocaine and nano iron tetroxide particles was visible under projection electron microscopy. Superparamagnetism experiments showed that the hysteresis lines were S-shaped and passed through the origin, and the microspheres were superparamagnetic. The in vitro release profile showed a slow and fast release, and the cumulative release of lidocaine reached 97 ± 1.97% at 60 h of sustained release, measured by UV indexing. This indicates that magnetic lidocaine is still released in small amounts after 60 h, supporting subsequent animal experiments. Kau

et al. [19] investigated the pattern of in vivo and in vitro release of Lidocaine–PLGA and found that within 4 days, in vivo release was lower (in nerves and synovial fluid) than in vitro and in muscle. From days 4–9, the concentration of in vivo release (in nerves and synovial fluid) was higher than that in vitro. Similarly, Hsu et al. [11] found a more stable concentration of Lidocaine–PLGA in rabbit tissues over a period of 3 days. These studies suggest inconsistent release rates in vivo and in vitro. This may explain why the in vitro release profiles are not in complete agreement with the results of animal experiments. In previous studies, the duration of analgesia in extended-release formulations was mostly within 48 h [20–22]. In contrast, the duration of analgesia in magnetic lidocaine microsphere formulations was up to 62 h, providing an effective method for postoperative analgesia.

PLGA is a polymer with good histocompatibility and biodegradability; it can be hydrolyzed and metabolized to lactic acid and glycolic acid in vivo through various tissue interactions, and finally metabolized to water and carbon dioxide and excreted [23–25]. PLGA can also be used as a drug carrier for neuroprotection and repair [26, 27]. This demonstrates the safety, reliability, and non-toxicity of PLGA as an injectable drug shell. Magnetic lidocaine microspheres show similar analgesic duration to marketed products, such as liposomal bupivacaine (EXPAREL®) [28] and bupivacaine/meloxicam (ZYNRELEF®) [29]. In addition, Fe_3O_4 is a drug carrier that contains biologically active components that can be metabolically converted to cell-available ferric ions through normal biochemical pathways. It also has excellent biological efficacy (including biocompatibility, surface activity, MRI, and degradability) and fewer adverse effects [30, 31].

In the therapeutic management of chronic pain, there is a focus on addressing innovative proposals for intraoperative and perioperative pain. Physicians and patients expect to reduce wound pain and recover earlier after surgery [32, 33]. This study demonstrates for the first time that magnetic lidocaine microspheres can be immobilized around or distributed along targeted nerves by magnetic dressings applied to the skin, avoiding premature diffusion into surrounding tissues and thus reducing analgesic effects. This may be a more effective way to treat postoperative pain and chronic pain.

Using the MRI capability of Fe_3O_4–PLGA microspheres, researchers have developed a number of tumor-targeting drugs [33, 34]. Previous studies have also demonstrated that Fe_3O_4–PLGA microspheres have excellent T2-weighted MRI properties [35]. In MRI experiments, we observed the morphology of magnetic lidocaine microspheres in vivo, demonstrating a certain neuroanchoring effect of the preparation. It acted longer around the nerve than other preparations without magnetic field attraction [10, 11]. This conjecture was further verified by peripheral nerve block experiments and analgesic experiments. Our animal experiments have shown that magnetic lidocaine microspheres prolong the duration of sciatic nerve block in rabbits, causing a decrease in sciatic nerve conduction velocity and action potential amplitude within 62 h. The duration of the nerve blocking effect of this preparation was lengthened significantly in comparison to the magnetic field-free group.

Previously, local anesthetics loaded on other materials provided continuous analgesia for 24–48 h [36]. However, the analgesic experimental studies showed that magnetic lidocaine microspheres prolonged the inhibition time of CTMR response in rats, significantly inhibiting the CTMR response within 62 h. In contrast, the magnetic field-free group significantly inhibited the CTMR response only within 36 h. In addition, the formulation extended the response time to thermal stimulation-induced acute pain in the right hind plantar region of rats to 64 h. In short, magnetic lidocaine microspheres may be able to provide longer analgesia in the presence of a magnetic field.

The present study has some limitations. The encapsulation rate of magnetic lidocaine microspheres prepared in this experiment remains to be optimized, and we formulated to improve it in future studies. This can be achieved via the optimization of microsphere morphology and the use of bilayer microsphere structure, which can also reduce the sudden release rate of the drug. In addition, the pharmacokinetics and peripheral magnetic field was designed for magnetic lidocaine microspheres require further investigation. Furthermore, we used a simple homemade version of the magnetic dressing, but the clinical application requires further consideration of the magnetic field strength to penetrate deeper into various tissues. This may require more individualized magnetic field designs and magnetic dressings with different field strengths.

Conclusion

In summary, this study showed that the prepared magnetic lidocaine microspheres were superparamagnetic, could anchor around nerves by magnetic fields on the body surface. Magnetic lidocaine microspheres achieved a cumulative release rate of 97% after 60 h in an in vitro release assay. Peripheral nerve block experiments and analgesic experiments revealed that magnetic lidocaine microspheres could be immobilized around nerves by a magnetic field, reducing diffusion and thus prolonging nerve block and analgesia, in comparison to lidocaine microspheres without magnetic field action. Fe_3O_4–local anesthetic–PLGA microspheres may be a new effective modality for the treatment of chronic pain.

Supplementary Information The online version contains supplementary material available at https://doi.org/10.1007/s00540-023-03305-1.

Acknowledgements This work was supported by grants from the Medical Science and Technology Project of Sichuan Provincial Health Commission (21PJ142) and the Chengdu Municipal Health Commission (2022167).

Author contributions LZ: This author helped conduct the experiments, analyze the statistics and write the article. QY: This author helped perform experiments. QL: This author helped perform experiments. CZ: This author helped design the study and provided experimental guidance.

Funding Health Commission of Sichuan Province, 21PJ142, Chuandong Zheng.

Data availability Data available on request from the authors. The data that support the findings of this study are available from the corresponding author, CZ, upon reasonable request.

Declarations

Conflict of interest The authors declare that they have no conflict of interest.

References

1. Coppens SJR, Zawodny Z, Dewinter G, Neyrinck A, Balocco AL, Rex S. In search of the Holy Grail: poisons and extended release local anesthetics. Best Pract Res Clin Anaesthesiol. 2019;33(1):3–21.
2. Ayyanaar S, Kesavan MP. Magnetic iron oxide nanoparticles@ lecithin/poly (l-lactic acid) microspheres for targeted drug release in cancer therapy [published online ahead of print, 2023 Oct 18]. Int J Biol Macromol. 2023;253(Pt 7):127480.
3. Ben-Akiva E, Karlsson J, Hemmati S, Yu H, Tzeng SY, Pardoll DM, Green JJ. Biodegradable lipophilic polymeric mRNA nanoparticles for ligand-free targeting of splenic dendritic cells for cancer vaccination. Proc Natl Acad Sci U S A. 2023;120(26):e2301606120.
4. Li H, Zhang X, Zhao W, Cai F, Qin J, Tian J. Efficacy of CalliSpheres® microspheres versus conventional transarterial chemoembolization in the treatment of refractory colorectal cancer liver metastasis. BMC Cancer. 2023;23(1):970.
5. Korde BA, Mankar JS, Phule S, Krupadam RJ. Nanoporous imprinted polymers (nanoMIPs) for controlled release of cancer drug. Mater Sci Eng C Mater Biol Appl. 2019;99:222–30.
6. Wang C, Zeng Y, Chen KF, Lin J, Yuan Q, Jiang X, Wu G, Wang F, Jia YG, Li W. A self-monitoring microneedle patch for light-controlled synergistic treatment of melanoma. Bioact Mater. 2023;27:58–71.
7. Kumbhar PS, Manjappa AS, Shah RR, Nadaf SJ, Disouza JI. Nanostructured lipid carrier-based gel for repurposing simvastatin in localized treatment of breast cancer: formulation design, development, and in vitro and in vivo characterization. AAPS PharmSciTech. 2023;24(5):106.
8. Zhou L, Feng W, Mao Y, Chen Y, Zhang X. Nanoengineered sonosensitive platelets for synergistically augmented sonodynamic tumor therapy by glutamine deprivation and cascading thrombosis. Bioact Mater. 2022;24:26–36.
9. Xu X, Chang S, Zhang X, Hou T, Yao H, Zhang S, Zhu Y, Cui X, Wang X. Fabrication of a controlled-release delivery system for relieving sciatica nerve pain using an ultrasound-responsive microcapsule. Front Bioeng Biotechnol. 2022;10:1072205.
10. Xu Q, Chin SE, Wang CH, Pack DW. Mechanism of drug release from double-walled PDLLA(PLGA) microspheres. Biomaterials. 2013;34(15):3902–11.
11. Hsu YH, Chen DW, Li MJ, Yu YH, Chou YC, Liu SJ. Sustained delivery of analgesic and antimicrobial agents to knee joint by direct injections of electrosprayed multipharmaceutical-loaded nano/microparticles. Polymers (Basel). 2018;10(8):890.
12. Guo Y, Logan HL, Glueck DH, Muller KE. Selecting a sample size for studies with repeated measures. BMC Med Res Methodol. 2013;13:100.
13. Lipengolts AA, Finogenova YA, Skribitsky VA, Shpakova KE, Anaki A, Motiei M, Semkina AS, Abakumov MA, Smirnova AV, Grigorieva EY, Popovtzer R. CT and MRI Imaging of Theranostic Bimodal Fe3O4@Au NanoParticles in Tumor Bearing Mice. Int J Mol Sci. 2022;24(1):70.
14. Yamasaki T, Fujiwara H, Oda R, Mikami Y, Ikeda T, Nagae M, Shirai T, Morisaki S, Ikoma K, Masugi-Tokita M, Yamada K. In vivo evaluation of rabbit sciatic nerve regeneration with diffusion tensor imaging (DTI): correlations with histology and behavior. Magn Reson Imaging. 2015;33(1):95–101.
15. Chou AK, Chiu CC, Chen YW, Wang JJ, Hung CH. Phentolamine reverses epinephrine-enhanced skin antinociception of dibucaine in rats. Anesth Analg. 2019;128(6):1336–43.
16. Tzeng JI, Wang JN, Wang JJ, Chen YW, Hung CH. Cutaneous synergistic analgesia of bupivacaine in combination with dopamine in rats. Neurosci Lett. 2016;620:88–92.
17. Wang J, Helder L, Shao J, Jansen JA, Yang M, Yang F. Encapsulation and release of doxycycline from electrospray-generated PLGA microspheres: effect of polymer end groups. Int J Pharm. 2019;564:1–9.
18. Malpezzi-Marinho ELA, Zanoni CIS, Molska GR, Paraventi C, Wuo-Silva R, Berro LF, Parada CA, Tamura EK, Marinho EA. Antinociceptive Activity of the Skin Secretion of Phyllomedusa rohdei (Amphibia, Anura). Toxins (Basel). 2020;12(9):589.
19. Kau YC, Liao CC, Chen YC, Liu SJ. Sustained release of lidocaine from solvent-free biodegradable poly[(d,l)-Lactide-co-Glycolide] (PLGA): in vitro and in vivo study. materials (Basel). 2014;7(9):6660–76.
20. Zhang X, Dang M, Zhang W, Lei Y, Zhou W. Sustained delivery of prilocaine and lidocaine using depot microemulsion system: in vitro, ex vivo and in vivo animal studies. Drug Dev Ind Pharm. 2020;46(2):264–71.
21. Svirskis D, Chandramouli K, Bhusal P, Wu Z, Alphonso J, Chow J, Patel D, Ramakrishna R, Yeo SJ, Stowers R, Hill A. Injectable thermosensitive gelling delivery system for the sustained release of lidocaine [published correction appears in Ther Deliv. 2016;7(7):511]. Ther Deliv. 2016;7(6):359–68.
22. Bnyan R, Khan I, Ehtezazi T, Saleem I, Gordon S, O'Neill F, Roberts M. Formulation and optimisation of novel transfersomes for sustained release of local anaesthetic. Pharm Pharmacol. 2019;71(10):1508–19.
23. Wen K, Na X, Yuan M, Bazybek N, Li X, Wei Y, Ma G. Preparation of novel ropivacaine hydrochloride-loaded PLGA microspheres based on post-loading mode and efficacy evaluation. Colloids Surf B Biointerfaces. 2022;210:112215.
24. Essa D, Kondiah PPD, Choonara YE, Pillay V. The design of poly(lactide-co-glycolide) nanocarriers for medical applications. Front Bioeng Biotechnol. 2020;8:48.
25. Su Y, Liu J, Tan S, Liu W, Wang R, Chen C. PLGA sustained-release microspheres loaded with an insoluble small-molecule drug: microfluidic-based preparation, optimization, characterization, and evaluation *in vitro* and *in vivo*. Drug Deliv. 2022;29(1):1437–46.

26. Zhu W, Chen L, Wu Z, Li W, Liu X, Wang Y, Guo M, Ito Y, Wang L, Zhang P, Wang H. Bioorthogonal DOPA-NGF activated tissue engineering microunits for recovery from traumatic brain injury by microenvironment regulation. Acta Biomater. 2022;150:67–82.
27. Manto KM, Govindappa PK, Martinazzi B, Han A, Hegarty JP, Koroneos Z, Talukder MH, Elfar JC. Erythropoietin-PLGA-PEG as a local treatment to promote functional recovery and neurovascular regeneration after peripheral nerve injury. J Nanobiotechnol. 2022;20(1):461.
28. Yu M, Yuan W, Xia Z, Liu Y, Wang Y, Xu X, Zheng J, Schwendeman A. Characterization of exparel bupivacaine multivesicular liposomes. Int J Pharm. 2023;639:122952.
29. Blair HA. Bupivacaine/meloxicam prolonged release: a review in postoperative pain. Drugs. 2021;81(10):1203–11.
30. Vangijzegem T, Stanicki D, Laurent S. Magnetic iron oxide nanoparticles for drug delivery: applications and characteristics. Expert Opin Drug Deliv. 2019;16(1):69–78.
31. Zhao S, Yu X, Qian Y, Chen W, Shen J. Multifunctional magnetic iron oxide nanoparticles: an advanced platform for cancer theranostics. Theranostics. 2020;10(14):6278–309.
32. Wainwright TW, Gill M, Mcdonald DA, Middleton RG, Reed M, Sahota O, Yates P, Ljungqvist O. Consensus statement for perioperative care in total hip replacement and total knee replacement surgery: Enhanced Recovery After Surgery (ERAS®) Society recommendations. Acta Orthop. 2020;91(1):3–19.
33. Frassanito L, Vergari A, Nestorini R, Cerulli G, Placella G, Pace V. Enhanced recovery after surgery (ERAS) in hip and knee replacement surgery: description of a multidisciplinary program to improve management of the patients undergoing major orthopedic surgery. Musculoskelet Surg. 2020;104(1):87–92.
34. Chen Q, Ma X, Xie L, Chen W, Xu Z, Song E, Zhu X, Song Y. Iron-based nanoparticles for MR imaging-guided ferroptosis in combination with photodynamic therapy to enhance cancer treatment. Nanoscale. 2021;13(9):4855–70.
35. Tousi MS, Sepehri H, Khoee S, Farimani MM, Delphi L, Mansourizadeh F. Evaluation of apoptotic effects of mPEG-b-PLGA coated iron oxide nanoparticles as a eupatorin carrier on DU-145 and LNCaP human prostate cancer cell lines. J Pharm Anal. 2021;11(1):108–21.
36. Peng F, Liu J, Zhang Y, Fan J, Gong D, He L, Zhang W, Qiu F. Designer self-assembling peptide nanofibers induce biomineralization of lidocaine for slow-release and prolonged analgesia. Acta Biomater. 2022;146:66–79.